

# Reduce energy consumption and improve efficiency in maritime operations

João Colares Costa Gaspar do Nascimento  
joao.c.nascimento@tecnico.ulisboa.pt

Instituto Superior Técnico, Lisboa, Portugal

September 2024

## Abstract

The shipping industry is responsible for a significant proportion of Greenhouse Gas (GHG) emissions. Over 90% of world trade is carried by 90,000 marine vessels, together producing more than 3% of global CO<sub>2</sub> emissions, and is expected to continue growing. Consequently, recent regulations are forcing this market to report their equipment energy and environmental efficiency, like the 2022 European Carbon Intensity Indicator (CII). This creates a strong need to implement new technologies for data capture and processing, report generation, and operational efficiency analysis. Sensors gather real-time data, which is analyzed and adjusted for the influence of external factors.

This thesis aims to define and implement Key Performance Indicators (KPIs) to capture various aspects of ship operations, providing critical information to enhance overall efficiency. Methodologies developed for the analysis incorporate models to estimate non-measured signals and the necessary corrections to ensure data quality. These approaches intend to enable effective monitoring of energy usage, facilitating comprehensive performance tracking, early detection of consumption degradation, and active energy management, in order to cut operational costs and to address the industry's need for environmental efficiency and regulatory compliance. These KPIs can be integrated into a tool to assist ship crews, management companies, and owners in making better decisions and receiving real-time notifications of any negative trends or overall performance issues.

**Keywords:** Data analysis; Energy efficiency; Energy management; Environmental compliance; Key performance indicators; Maritime operations;

## 1. Introduction

Nowadays, shipping represents over 80% of world trade due to their reliability and ability to adapt to any type of cargo. In 2021, shipments grew by an estimated 3.2%, reaching 11 billion metric tons (MT) of cargo [1]. Due to this increase, the total shipping GHG emissions have increased from 977 million MT of CO<sub>2</sub> eq. in 2012 to 1,076 million MT of CO<sub>2</sub> eq. in 2018, representing a 10% increase. The share of shipping emissions in global emissions has increased from 2.76% in 2012 to 2.89% in 2018 [2]. Since 2012, when analyzing exclusively the CO<sub>2</sub> emissions, the general trend shows an average annual increase of approximately 2.5% CO<sub>2</sub> emissions, surpassing 850 million MT [3]. The fleet's average age is also rising, which represents a challenge for modernization and a concern since older ships tend to pollute more. [1].

Recent regulations are forcing this market to report their equipment energy and environmental efficiency. As a stimulus to reduce carbon intensity of all ships by 40% by 2030 compared to 2008 base-

line, operators will be required to register certain metrics, such as the annual operational CII. The requirements for its certification came into effect on 1 January 2023 [4].

In this context, collecting real-time data and analyzing relevant KPIs is useful to identify performance issues caused by wear-affected components and possible improvements. This analysis, along with the need for power correction to account for weather factors, results in a more in-depth understanding of the vessel's energy efficiency and behavior under varying conditions.

For this purpose, this study is performed in collaboration with Nortech AI which is a startup specialized in Industrial IoT solutions, including in the maritime industry, from collecting sensor data to deploying anomaly detection and predictive maintenance models. The selected KPIs study can be developed using their real-world data and, ultimately, be implemented in a tool to support operators in strategic planning to achieve significant financial and environmental impact.

## 2. Background and State of the Art

### 2.1. Vessel's KPIs

This thesis will approach 5 specific KPIs that collectively offer a perspective on the vessel performance optimization for both economic efficiency and environmental sustainability: CII, slip, fuel performance, trim, and hull and propeller performance.

#### 2.1.1. CII

The CII is a measure that attempts to quantify the environmental efficiency of a ship. It takes into account CO<sub>2</sub> emissions, linking those CO<sub>2</sub> emissions to the amount of cargo carried over distance travelled. The annual operational CII is generically attained as follows [4]:

$$CII_{Ship} = \frac{M}{C \cdot D_t} \quad (1)$$

where:

- $M$  [g] - total mass of CO<sub>2</sub> emitted;
- $C$  [MT] - ship's capacity;
- $D_t$  [nautical miles] - distance travelled.

The attained CII,  $CII_{Ship}$ , is then verified against the required value,  $CII_{Req}$ , corresponding to the same calendar year, expressed in equation 2:

$$CII_{Req} = \left(1 - \frac{Z}{100}\right) \cdot CII_{Ref} \quad (2)$$

where  $Z = \{ 5\% \text{ for } 2023; 7\% \text{ for } 2024; 9\% \text{ for } 2025; 11\% \text{ for } 2026 \}$  are the reduction factors that force the  $CII_{Req}$  for a ship to become more stringent over the years [4]. This reduction factor is then used against the reference value ( $CII_{Ref}$ ), from the reference year of 2019. For each ship,  $CII_{Ref}$  is attained as follows:

$$CII_{Ref} = a \cdot Capacity^{-c} \quad (3)$$

where  $a$  and  $c$  are parameters estimated through median regression, tabulated according to ship type [4], and  $Capacity$  is the ship's capacity in MT.

According to a ship's CII, its carbon intensity will be rated based on a five-grade rating mechanism composed of following grades: A, B, C, D, or E. The grades are attained as a function of  $CII_{Req}$  [4]. A ship is considered non-compliant if it scores E for one year or D for three consecutive years.

#### 2.1.2. Slip

The propeller is attached to a shaft and will propel the ship forward. Propeller pitch is the distance the propeller would move forward in one rotation. Slip

represents the difference between the distance traversed by the ship through water in one shaft rotation and the anticipated distance based on the angle of attack of its blades (equation 4).

$$\text{Slip [\%]} = \frac{(\text{Propeller dist.}) - (\text{Ship dist.})}{\text{Propeller dist.}} \cdot 100 \quad (4)$$

where:

$$\text{Propeller dist. [NM]} = \frac{\text{Pitch} \cdot \text{RPM} \cdot 60}{1852} \quad (5)$$

considering that  $Pitch$  is a characteristic of each specific propeller and that one nautical mile (NM) is approximately equal to 1852 meters.

#### 2.1.3. Fuel Performance

Engine's efficiency in converting fuel to energy is crucial for optimizing fuel consumption, thus reducing operational costs and environmental impact.

Gkerekos et al. (2019) [5] presented a comparative study of data-driven, multiple regression algorithms for predicting main engine's consumption considering two different shipboard data acquisition strategies, noon-reports and continuous data monitoring systems. The study concludes that continuous data monitoring systems can enhance modelling by 7% compared to noon-reports.

#### 2.1.4. Trim

The vessel has a draft,  $t_f$ , measured at the forward end and a draft value,  $t_a$ , measured at the aft end. Total trim is given by  $t = t_f - t_a$ . Trimming is not always disadvantageous as intentionally inducing a certain degree of trim by bow or stern within specific limits can enhance efficiency and reduce emissions.

By actively planning cargo loading one can optimize the trim and draft. The Global Maritime Energy Efficiency Partnerships [6] estimates trim optimization to reduce the fuel consumption by 0.5% to 3% for most ship types, although for ships which often trade in partial load conditions the effect can be up to 5%.

The Asian Maritime Technology Cooperation Centre [7] introduces the operations of ship trim optimization based on the machine learning method, including the data preparation, system development and practical cases. It presents three case studies in which fuel savings up to 5% less are obtained.

#### 2.1.5. Hull and Propeller Performance

Hull performance is a vital metric in marine engineering, encapsulating the efficiency with which a

ship moves through water. As a vessel navigates through water, its hull becomes a breeding ground for biological growth, a phenomenon referred to as fouling. This accumulation, along with any other possible damage, diminish the hull's smoothness, escalating the friction between the vessel and the surrounding water. Consequently, there is an increase in the ship's power demand. On average, hull fouling elevates the power required by an individual ship by approximately 7%, with variations ranging from 2% to 11%, largely influenced by the vessel's age and its maintenance practices [8].

In order to quantify this performance, one can estimate the ideal speed derived from the power delivered by the ship's main engine and other relevant parameters. This predicted speed value is then compared against the actual measured value of speed. Evidently, this speed loss is expected to increase over time due to accumulated wear and damage, indicating the need to clean and/or repair the hull and the propeller. The change in hull and propeller performance measured before and after a maintenance event can be used to determine the effectiveness of said maintenance [9].

## 2.2. Corrections

Ship speed trials provide valuable data on the ship's propulsion system, engine performance, and overall hydrodynamic characteristics. These trials are conducted by navigating the ship through a series of tests in open waters under stipulated conditions: smooth propeller surfaces, no wind, no waves, no current and deep water of 15°C [10]. It cannot be expected that such conditions will always be met during actual trials and corrections for the environmental conditions have to be considered. Consequently, these corrected results become ideal reference values.

The work by Prpić-Oršić and Faltinsen (2012) [11] involved detailed modeling of weather effects on the ship's added resistance and fuel consumption. Their findings indicate that, on average, a 15% increase in power demanded compared to calm water baseline can occur. Whilst simplistic, this assumption is applied as a starting assumption for the average increase in resistance for all ocean-going ship types, following the *Third IMO GHG Study 2014* (Smith et al., 2015) [12].

### 2.2.1. Generic procedure

Measured signals are obtained for real conditions, where several factors add up to the total in-service resistance that the vessel has to withstand during normal operation (equation 6).

$$R_T[N] = R_{drag} + R_{added} = R_{drag} + R_{AS} + R_{AA} + R_{AW} + R_{AH} \quad (6)$$

where:

- $R_T$  [N] - total in-service resistance;
- $R_{drag}$  [N] - resistance experienced by the vessel sailing through water;
- $R_{AS}$  [N] - resistance increase due to the deviation of water temperature and density;
- $R_{AA}$  [N] - resistance increase due to wind;
- $R_{AW}$  [N] - resistance increase due to waves;
- $R_{AH}$  [N] - resistance increase due to changes in hull condition.

According to ISO standards [9], the delivered power  $P_D$  can be expressed as:

$$P_D[\text{kW}] = \frac{R_T \cdot \text{Speed}}{\eta} \cdot \frac{0.514}{1000} \quad (7)$$

where the factor 0.514 converts the measured speed from knots to meters per second and  $\eta$  is the propulsive efficiency, which encompasses several components such as open-water efficiency, hull efficiency, relative rotative efficiency, and transmission efficiency. In this context, the delivered power to compensate the effect of the in-service non-ideal added resistance,  $\Delta P_D$ , can be expressed as:

$$\Delta P_D[\text{kW}] = \frac{R_{added} \cdot \text{Speed}}{\eta} \cdot 0.000514 \quad (8)$$

Finally, the corrected predicted power can be expressed as:

$$P_{D,corr} [\text{kW}] = P_D - \Delta P_D \quad (9)$$

When the propulsive efficiency coefficient is not available, the standard fixed value 0.7 should be assumed as proposed in ISO standards [13].

Additionally, from equation 8, the added resistance due to changes in hull condition can be expressed as:

$$R_{AH}[\text{N}] = \frac{\Delta P_D \cdot \eta}{\text{Speed} \cdot 0.000514} - (R_{added} - R_{AH}) \quad (10)$$

### 2.2.2. Power Correction for Wind Resistance

According to ISO [13], true wind velocity,  $v_{wt}$  (m/s), and true wind direction,  $\Psi_{wt}$  (°), at height of the anemometer, are computed from: the relative wind velocity, the vessel's speed over ground, direction

of the relative wind, and the vessel's heading. From  $v_{wt}$  and  $\Psi_{wt}$ , it is possible to compute the relative wind velocity and direction at reference height,  $v_{wr,ref}$  (m/s) and  $\Psi_{wr,ref}$  ( $^\circ$ ), respectively.

From equations 8 and 6, the power wind correction can be derived as:

$$\Delta P_{AA}[kW] = \frac{R_{AA} \cdot Speed}{\eta} \cdot 0.000514 \quad (11)$$

According to ISO [10], Annex C, resistance increase due to wind is calculated as follows:

$$R_{AA} = R_{rw} - R_{0w} = (0.5\rho_A C_{AA}(\Psi_{wr,ref}) A_{XV} v_{wr,ref}^2) - (0.5\rho_A C_{AA}(0) A_{XV} v_g^2) \quad (12)$$

where:

- $A_{XV}$  [m<sup>2</sup>] - transverse projected area above the waterline including superstructures;
- $C_{AA}$  - wind resistance coefficient;  $C_{AA}(0)$  - wind resistance coefficient in head wind;

In ISO standards [10],  $C_{AA}(\Psi_{wr,ref})$  regression formula based on wind tunnel tests developed by Fujiwara et al. [14] and the non-dimensional parameters that come from wind tunnel tests can be found. However, STA-JIP [15], provides a dataset of wind resistance coefficients obtained through various experiments. ISO [10] Annex C provides data for several types of ships.

### 2.2.3. Power Correction for Wave Resistance

From equations 8 and 6, the power wave correction can be derived:

$$\Delta P_{AW}[kW] = \frac{R_{AW} \cdot Speed}{\eta} \cdot \frac{0.514}{1000} \quad (13)$$

According to ISO [10], Annex D, resistance increase due to waves can be estimated as described in equation 14. This is a simplified model which is restricted to waves in the bow sector.

$$R_{AWL} = \frac{1}{16} g \rho_S H_{1/3}^2 B \sqrt{\frac{B}{L_{BWL}}} \quad (14)$$

where:

- $\rho_S$  [kg/m<sup>3</sup>] - water density;
- $g$  [m/s<sup>2</sup>] - acceleration of gravity;
- $H_{1/3}$  [m] - significant wave height;
- $B$  [m] - Breadth;
- $L_{BWL}$  [m] - Distance between the bow and 95% of maximum breadth on the waterline;

with the additional restriction:

$$H_{1/3} \leq 2.25 \cdot \sqrt{\frac{L_{PP}}{100}} \quad (15)$$

## 3. Methodology

To perform KPI analysis, it is necessary to collect real data and to develop several estimation models. Data is collected either from Automatic Identification System (AIS) or through continuous onboard measurement. Speed and power data are crucial for developing the selected KPIs. The vessel's actual speed measurement is needed for most KPIs, as they depend on it, while power can be estimated. The speed model is designed to simulate ideal conditions but it does not estimate real speed. Although the methodology is implemented using real data, the results and validation of the proposed methods are the focus of Section 4.

### 3.1. Available Data

For this study, Nortech AI provided data from two different Bulk Carrier vessels, here defined as Vessel A and Vessel B, for confidentiality purposes. The main vessel characteristics are summarized in Table 1 and include: the length overall including any projections,  $L_{OA}$ , the length between perpendiculars excluding any overhanging projections,  $L_{PP}$ , the width measured at its widest point,  $Breadth$ , the vertical distance from the baseline to the uppermost point of the deck,  $Depth$ , the predetermined vertical distance from the waterline to the keel,  $designed\ draft$ , the volume of all enclosed spaces on a vessel,  $Gross\ Tonnage$ , and the maximum weight it can carry during summer months,  $Summer\ DWT$ . Additionally, the table includes designations of each engine, along with each vessel's nominal power and speed. Technical descriptions of these engines is described in more detail in the manufacturer's manuals [16].

	Vessel A	Vessel B
$L_{OA}$ [m]	229.99	299.95
$L_{PP}$ [m]	226.15	294.40
Breadth [m]	32.26	50.00
Depth [m]	20.00	24.90
Designed draft [m]	12.20	16.10
Gross tonnage [MT]	43229	107879
Summer DWT [MT]	81085	208445
Engine designation	G70ME-C9.2	6S60ME-C8.2
Nominal Power [kW]	8881	15131
Nominal Speed [knots]	16.12	14.50

**Table 1:** Comparison between Vessel A and Vessel B main characteristics

Furthermore, Table 2 establishes the mapping between available signals and use case vessels. The source of each signal is categorized into two distinct types: continuous onboard measurement and AIS.

Selected signals	Vessel A	Vessel B
Power	-	Measured
Speed	Measured	AIS
Draft	AIS	Measured
Trim	AIS	Measured
Fuel consumption	-	Measured
Wind	Measured	AIS
Waves	AIS	AIS
Weather (other)	-	AIS

**Table 2:** Mapping of selected signals, measured onboard or collected from AIS, for each use case vessel

### 3.2. Power Models

To construct the power estimation models, an analysis of data obtained from the engine shop trial is conducted. The engine shop trial involves tests carried out on the ship's engine within the controlled environment of a designated workshop.

Regression models were developed to estimate power output for Vessel B. The engine trial data served as the training dataset for model development. Measured real-time power output data, filtered to remove outliers and transient periods, was used for comparison.

The models were constructed for every possible combination of features. Engine's intrinsic signals were selected based on their presence in both vessels' engine trials and measurement systems. This approach aimed to ensure consistency across vessels and enable the use of the same model inputs, which yielded better results when training for Vessel B, to predict power for Vessel A. To select the model, the comparison with real values was performed through the computation of several error metrics such as Mean Absolute Error (MAE), Root Mean Squared Error (RMSE) and Mean Absolute Percentage Error (MAPE). The selected model, presented a MAPE accuracy of approximately 3% for Vessel B's available dataset and is represented by equation 16:

$$\text{Power Output [kW]} = \alpha_0 + \sum_{k=1}^4 \alpha_k T C^k \quad (16)$$

### 3.3. Speed Models

MATLAB Curve Fitter tool is employed to analyze diverse sets of speed and power vectors, each corresponding to a constant draft value. This data was retrieved from the Vessel A's Speed Trial results. In this context, the Polynomial Surface Fit, in which  $f(x, y)$  represents speed, is accomplished by equation 17, and its representation is shown in Figure 1.

$$f(x, y) = p_{00} + p_{10}x + p_{01}y + p_{20}x^2 + p_{11}xy + p_{30}x^3 + p_{21}x^2y + p_{40}x^4 + p_{31}x^3y \quad (17)$$

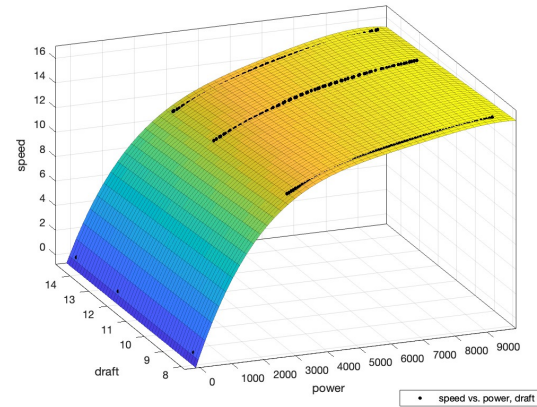


**Figure 1:** Vessel A's 3D Speed Power Curves

### 3.4. Power Correction for Hull and Propeller Performance

The developed speed model based on speed trial data, corrected for wind, wave, and current is employed. However, the registered vessel speed corresponds to real operating conditions. Therefore, this approach requires computing the added resistance attributed to wind and waves, defined in equations 11 and 13, respectively. After correcting the consumed power for the aforementioned effects, any disparity between predicted and actual speed primarily reflects the resistance increase resulting from hull condition changes, as detailed in equation 6. Tracking speed loss percentages over time offers insights into hull and propeller condition evolution.

## 4. Models Results

### 4.1. Power Models

Vessel A lacks direct power measurement. Hence, the assessment was conducted in terms of fuel consumption. Since fuel consumption data is not available for Vessel A, an estimation was required. To facilitate this estimation, the fuel consumption was derived from the power output prediction using an SFOC model, which is based on the engine's trial data and graphically represented in Figure 2. Using the SFOC model, it is possible to compare estimated and actual fuel consumption [MT], provided that noon reports from an equivalent period are available. This fuel consumption analysis, which encompasses both the power and the SFOC models, yielded a MAE of 2.76 MT, and a cumulative MAPE of 2.50% over a six-month period.

### 4.2. Speed Models

Given that the models are derived from idealized behavior, the estimated speed is anticipated to consistently surpass the actual speed. The trial results of the ship are corrected for wind, waves, and current, consequently, the predictions are com-

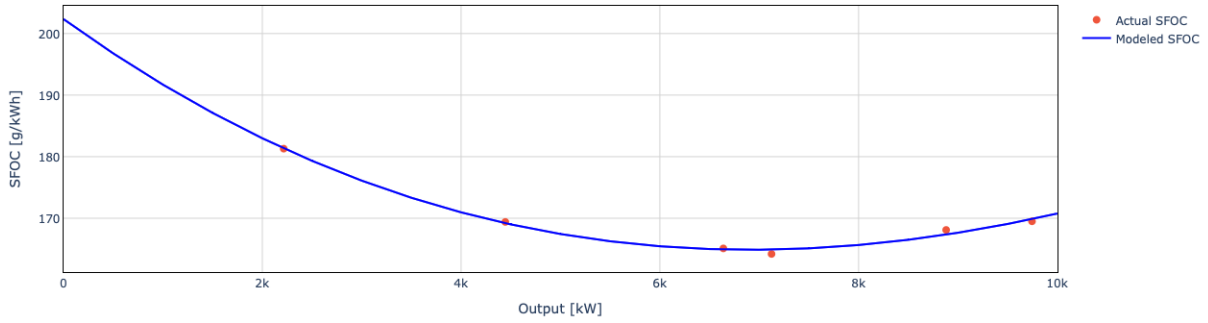


Figure 2: Vessel A's SFOC model created from engine trial data

pared against the ship's actual speed through water (STW), as this value discounts the influence of currents during normal operation, unlike the speed over ground (SOG).

#### 4.3. Power and Speed Corrections

In ship design, it is standard practice to assume a sea margin of 15% on power demand to account for performance loss due to wind and waves [17]. Nevertheless, various methods exist to address this issue, as discussed in Section 2.2.

##### 4.3.1. Wind Correction

ISO 15016 [10] delineates two empirical methodologies for forecasting wind resistance: the STA-JIP method [15] and the Fujiwara method [14]. Fujiwara is overall more complex to implement and dependent on detailed ship's structure information. Additionally, the Blendermann method [18] is widely applied in the literature. The average added resistance from STA-JIP and Blendermann methods is applied, as it is expected to provide a reliable prediction.

##### 4.3.2. Waves Correction

STA-1 method is employed, as it is recommended in ISO 15016 [10] and generally applicable across various ship types. However, STA-1 is restricted to waves in the bow sector and mild sea states.

##### 4.3.3. Wind and Waves Correction

Corrections for wind and waves were applied simultaneously and compared in terms of additional power demand as a percentage of total engine output. Wind correction averaged a 2.41% increase in power, while wave correction averaged 14.43%. In terms of speed, the ideal speed derived from the proposed model presented an average deviation of 20.52% from the real speed through water. After corrections, the deviation dropped to 14.78%.

## 5. KPI Evaluation

### 5.1. CII

The parameters that define the reference lines specific to the different types of ships and integrate the calculation of  $CII_{Ref} = a \cdot Capacity^{-c}$  were obtained from the IMO guidelines [4].  $CII_{Req}$  undergoes annual updates by adjusting  $Z$  (equation 2). The grading boundaries are also updated annually, as they depend on the  $CII_{Req}$ .

To compute the actual value of CII, the first step is to compute the mass of  $CO_2$  released into the atmosphere as a function of fuel consumed. Consequently, it is dependent on the type of fuel that is being used. For a comparative analysis, possible types of fuel were selected: HFO, MDO and MGO and LFO. The comparison between those selected fuel types is presented in Table 3.

	$CO_2$ factor [g/g]	Density [MJ/kg]
HFO	3.114	40.2
LFO	3.151	41.2
MDO/MGO	3.206	42.7

Table 3: Emission factors and energy density of selected maritime fuels

The attained CII values, based on fuel consumption during sailing voyages, for Vessel A and Vessel B are compared against the thresholds for the five grades. This analysis is performed at 10-minute intervals, for a more detailed view, or cumulatively, to observe its evolution over an entire year. The values of CII are expected to be heavily affected by factors such as currents, weather conditions and auxiliary engines' fuel consumption. However, normalizing them for mid draft accounts for the increased power demand associated with higher drafts. This levels the values across different loading condition voyages, highlighting a significant weakness in the current CII rating system, which is computed without considering whether the ship is transporting cargo. Ultimately, it can provide a perverse incentive to maximizing ballast voyages, particularly for older and more polluting

ships, in order to correct their rating.

## 5.2. Fuel Performance

### 5.2.1. Fuel energy efficiency

Measuring or estimating the engine's power output and fuel consumption enables the fuel efficiency study, considering the specific fuel energy density defined in Table 3. Equation 18 quantifies the fuel energy conversion efficiency of the engine.

$$\text{Fuel efficiency [\%]} = \frac{\text{Engine output}}{\text{Fuel energy}} \cdot 100 \quad (18)$$

Combustion engines typically operate more efficiently at higher loads but at a decreasing rate as they approach their designed optimal operating range. For marine engines, this optimal point is usually within a specific range of the engine's maximum continuous rating (MCR), often around 70-85% of MCR. Since the direct measurement of power output and fuel consumption is available for Vessel B, it is possible to compare the engine's actual efficiency, derived from real fuel consumption, against the predicted efficiency, derived from an SFOC model. This comparison is depicted in Figure 3.

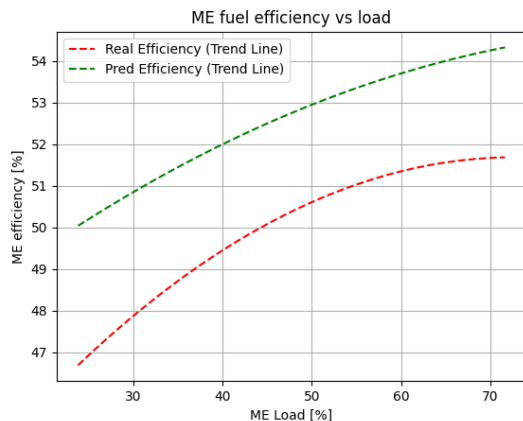


**Figure 3:** Comparison between the Vessel B's engine predicted and actual efficiency as a function of its load

The discrepancy between real and predicted efficiency can be attributed to several factors. The SFOC model is corrected for ISO conditions, which differ from real-world conditions. In actual operations, engine load varies more frequently, and factors like engine degradation, additional heat losses, and less precise measurement techniques contribute to lower real efficiency.

However, there were periods when the engine operated with an efficiency deviation of approximately 1% compared to the estimation derived from the SFOC model. Thus, an analysis was conducted to determine potential fuel savings if an op-

timal efficiency was maintained throughout the entire period. A maximum 2% efficiency offset relative to the ideally derived efficiency was defined arbitrarily assuming the model to be relatively accurate. This theoretical analysis yielded possible savings of 97 MT of fuel, corresponding to 3.15% fuel savings over a six-month period.

### 5.2.2. Fuel consumed per nautical mile

Vessel B tends to consume more fuel per NM than Vessel A, which can be explained primarily due to the higher nominal power of its engine. Furthermore, the fuel performance of both cases can be examined as a function of the vessel's STW, as depicted in Figures 4 (a) and (b), for Vessel A and Vessel B, respectively.

There is a clear trend indicating that as speed increases, fuel performance improves, since fuel consumption per NM decreases. This suggests that higher speeds are more fuel-efficient likely due to the engine operating closer to its optimal load point, while lower speeds may be a result of sub-optimal engine loading and varying sea and weather conditions. This analysis can serve as a support for slow steaming strategies, where ships deliberately reduce speed to cut fuel consumption and carbon emissions.

### 5.3. Slip

The difference between the actual distance a ship covers in water and the theoretical distance it should cover based on the propeller's rotations considering fixed pitch was calculated. The analysis focuses on real slip, considering the vessel's STW to exclude the effect of additional resistance caused by sea currents.

For each vessel, a six-month period was available for analysis. Vessel A presented an average slip value of 18.2%, compared to Vessel B's average value of 11.1%. Note that for Vessel B, AIS data was used, introducing higher error potential to the calculations.

Additionally, there is a visible positive correlation between real slip and attained CII, depicted in Figures 5 (a) and (b). This correlation is expected as increased slip typically means less efficient propulsion, leading to higher fuel consumption and consequently higher emissions per NM.

### 5.4. Hull and Propeller Performance

In this section, the isolation of the influence of hull and propeller defects on the overall ship performance is delineated. For this purpose, the corrections previously discussed are necessary to enable the tracking of error evolution over time, which is presumed to increase until a maintenance event occurs. After quantifying the influence of external

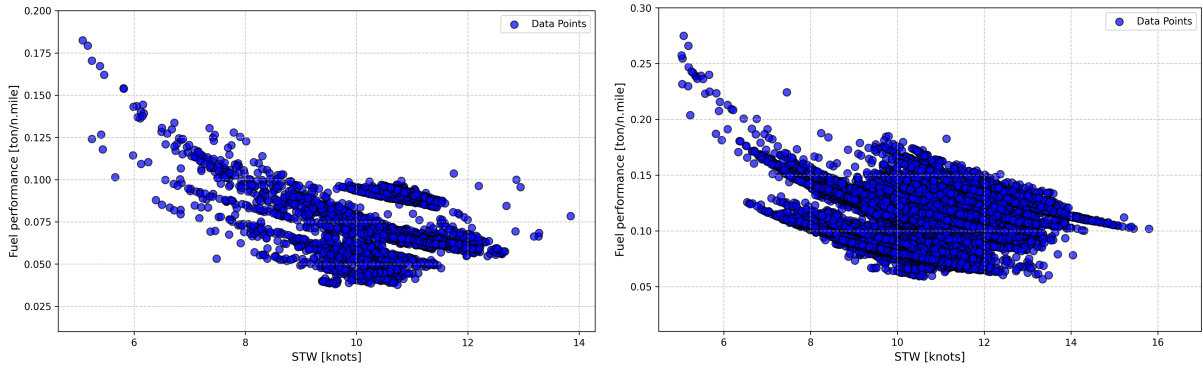


**Figure 4:** Main engine fuel consumption per nautical mile as a function of the ship's STW, considering: (a) estimated fuel consumption for Vessel A, (b) real fuel consumption Vessel B

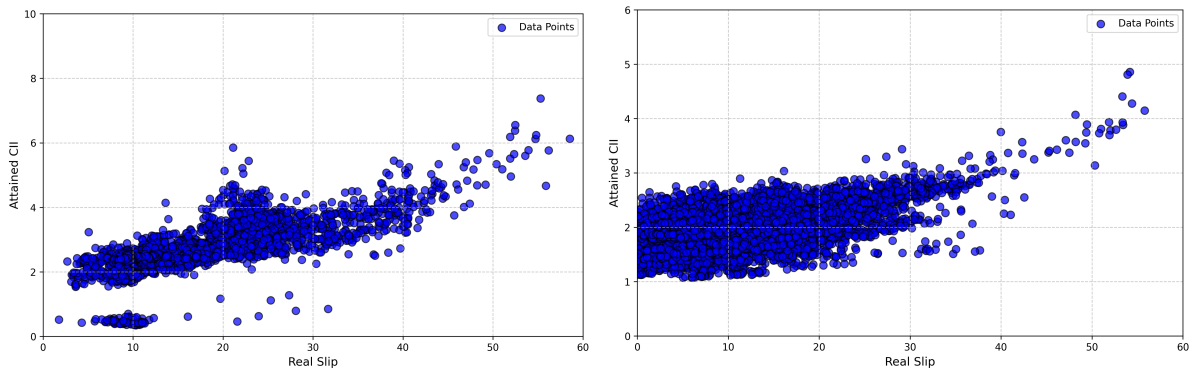


**Figure 5:** Attained CII as a function of real slip computed for: (a) Vessel A, (b) Vessel B

factors by computing and, subsequently, subtracting their added resistance, it is hypothesized that any remaining error can be attributed to errors in the models and performance degradation caused by hull and propeller fouling.

For both cases, when comparing predicted corrected speed against real speed, an apparent drop of 5% of speed loss occurs at a certain point of the analyzed time periods. Assuming the required power to be proportional to the cubic of the speed, it results in a reduction of approximately 14% of the engine's power demand. Evidently, to confirm this hypothesis, it is necessary to verify these results against the vessel's maintenance logs and determine if this identified drops correspond to a maintenance stoppage. Theoretically, with a larger dataset and more vessel data, it would be possible to determine average error offsets and to develop a pattern recognition model to optimize maintenance schedules.

### 5.5. Trim

Dynamic trim optimization includes real-time or intermittent adjustments while the ship is underway, ensuring optimal trim is maintained throughout the voyage. Using machine learning to optimize trim for fuel consumption offers key advantages:

greater accuracy, lower costs, and easier operation, provided there is sufficient high-quality historical navigational data. Additionally, machine learning enables self-learning and adaptation to the ship's voyage [7].

A random forest regressor model was implemented to understand how different features, such as speed, draft, and trim, influence the prediction of fuel consumption of the main engine of Vessel B when sailing under varying weather conditions.

After a data cleaning process, a total of 17,981 valid data sets were obtained, using a combination of onboard sensors and AIS sources. Inspection of the dataset demonstrates a clear clustering of data points, indicating two distinct operational regimes, as depicted in Figure 6.

Furthermore, while trim optimization can be more effective at deep drafts due to the greater potential for resistance reduction, at lower drafts there is a wider range of trims that result in efficient fuel consumption compared to the narrower range for higher drafts. This distribution introduces complexity into trim optimization. The presence of distinct clusters means that any strategy must account for varying operational regimes, making a one-size-fits-all solution challenging. Instead, optimization strategies may need to be tailored to specific draft

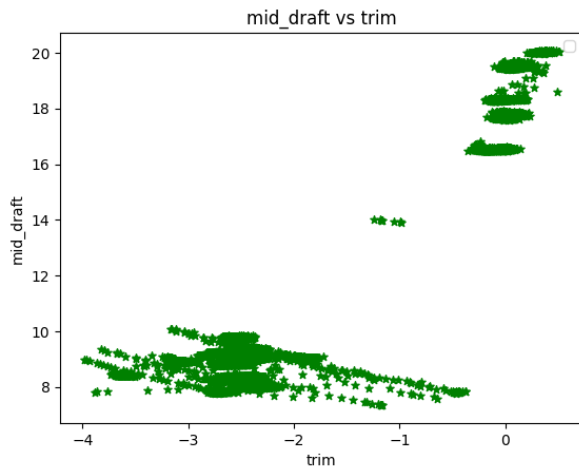


**Figure 6:** Scatter plot of mid draft vs. trim values for Vessel B

conditions to achieve optimal performance and fuel efficiency.

Feature selection was conducted using the Spearman Rank analysis to prevent the selection of redundant variables and to identify the most strongly correlated variables. In conclusion, the selected variables for the model to predict the fuel consumption are: STW, mid draft, trim, sea surface temperature, significant wave height, direction and period and wind speed and direction.

The dataset is randomly partitioned into training and testing subsets using an 80:20 split ratio. Within the training subset, hyperparameter tuning is conducted using *GridSearchCV* with *k-fold cross-validation*. Model results are illustrated in Figure 7.

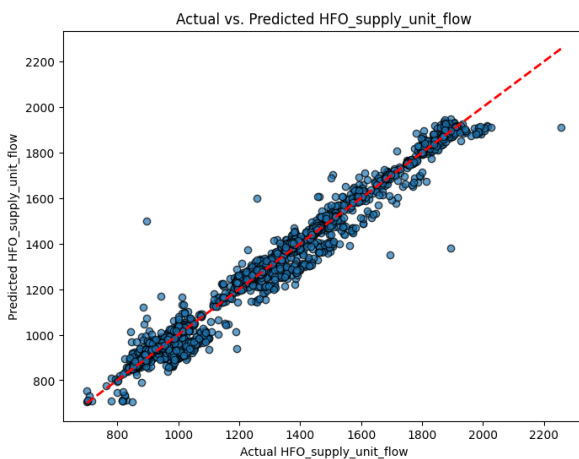


**Figure 7:** Scatter plot of actual vs. predicted fuel consumption for Vessel B

For actual fuel consumption values ranging from 800 to 2000 L/h, the model presents a MAE of 28.08 L/h and a MAPE of 2.41%. According to the model, mid draft, STW and trim are the most in-

fluential features affecting fuel consumption, while environmental factors have less impact on the predictions.

Subsequently, the model was used to predict fuel consumption for each data point collected, while maintaining all the inputs as they were recorded except for trim. Trim was varied by intervals of 0.25 meters, always considering the two cluster areas of operation restriction aforementioned. Using the model to compute dynamic optimal trim over the same six-month period suggests potential cumulative fuel savings of 90 MT, corresponding to 2.58% savings compared to the actual total fuel used during that period.

## 6. Conclusions and Future Work

This report proposes methodologies for ship performance analysis, focusing on selected KPIs. For that purpose, this work delved into the intricacies of power, speed, and fuel consumption modeling. The engine's power output was estimated using some of its intrinsic signals. Speed models were derived from speed trial curves, encompassing the relationship between speed, power, and mid draft. These speed models simulate ideal conditions and must be corrected for real-world conditions. Fuel consumption models are derived from SFOC curves registered during the engine trials.

However, the efficiency analysis in this study is constrained by the availability, quantity and quality of the data. Specifically, maintenance event records are needed to validate the hull and propeller performance against baseline values. Additionally, the accuracy of trim optimization would benefit significantly from larger and more representative datasets.

Future work should focus on implementing more complex and less restricted power corrections due to waves, as well as power corrections for water temperature and density. Moreover, a model such as gradient boosting should be studied to support incremental learning for trim optimization, allowing updates with new data without total retraining. Furthermore, a more comprehensive analysis of the engine's behavior and efficiency should be conducted.

Ultimately, the goal is that this work serves as a support to implement a tool that addresses various aspects of a vessel's operation, providing a comprehensive view of its overall efficiency. Nortech AI has already developed a production tool which can leverage these studied KPIs with real-time data. This implementation not only provides information to the operators but also has the potential to raise warnings and reveal opportunities for optimization. In turn, this can significantly contribute to reduce costs and global CO<sub>2</sub> emissions by the industry.

## References

- [1] Review of maritime transport 2022 | UNCTAD. [Online]. Available: <https://unctad.org/rmt2022>
- [2] Fourth greenhouse gas study 2020. [Online]. Available: <https://shorturl.at/xrIP8>
- [3] Insights - marine benchmark. [Online]. Available: <https://www.marinebenchmark.com/insights/>
- [4] Index of MEPC resolutions and guidelines related to MARPOL annex VI. [Online]. Available: <https://shorturl.at/S1X6J>
- [5] C. Gkerekos, I. Lazakis, and G. Theotokatos, "Machine learning models for predicting ship main engine fuel oil consumption: A comparative study," vol. 188, p. 106282.
- [6] Trim and draft optimization. [Online]. Available: <https://glomeep.imo.org/technology/trim-and-draft-optimization/>
- [7] MTCC-asia pilot projects. [Online]. Available: <https://gmn.imo.org/pilot-project/mtcc-asia-pilot-projects/>
- [8] N. Olmer, B. Comer, B. Roy, X. Mao, and D. Rutherford, "Greenhouse gas emissions from global shipping, 2013–2015 detailed methodology," *International Council on Clean Transportation: Washington, DC, USA*, pp. 1–38, 2017.
- [9] 14:00-17:00. ISO 19030-1:2016. [Online]. Available: <https://www.iso.org/standard/63774.html>
- [10] ——. ISO 15016:2015. [Online]. Available: <https://www.iso.org/standard/61902.html>
- [11] J. Prpić-Oršić and O. M. Faltinsen, "Estimation of ship speed loss and associated co2 emissions in a seaway," *Ocean Engineering*, vol. 44, pp. 1–10, 2012.
- [12] T. Smith, J. Jalkanen, B. Anderson, J. Corbett, J. Faber, S. Hanayama, E. O'Keeffe, S. Parker, L. Johansson, L. Aldous, C. Raucci, M. Traut, S. Ettinger, D. Nelissen, D. Lee, S. Ng, A. Agrawal, J. Winebrake, M. Hoen, and A. Pandey, *Third IMO GHG Study 2014: Executive Summary and Final Report*, 07 2014.
- [13] 14:00-17:00. ISO 19030-2:2016. [Online]. Available: <https://www.iso.org/standard/63775.html>
- [14] T. Fujiwara, M. Ueno, and Y. Ikeda, "Cruising performance of a large passenger ship in heavy sea." OnePetro.
- [15] H. van den Boom, H. Huisman, and F. Mennen, "New guidelines for speed/power trials level playing field established for IMO EEDI."
- [16] Two-stroke. [Online]. Available: <https://www.man-es.com/marine/products/two-stroke-engines>
- [17] Sub project 4 - performance in a seaway. [Online]. Available: <https://www.smartmaritime.no/sub-projects/sub-project-4-performance-in-a-seaway/>
- [18] W. Blendermann, "Estimation of wind loads on ships in wind with a strong gradient," in *OMAE*, vol. 1, 1995, pp. 271–277.